

2. Alexander, K. A. & Appel, M. J. G. *J. Wildl. Dis.* **30**, 481–485 (1994).
3. Macdonald, D. W. *Nature* **360**, 633–634 (1992).
4. Packer, C. & Pusey, A. E. *Am. Nat.* **145**, 833–841 (1995).
5. Packer, C. *et al. Reproductive Success* (ed. Clutton-Brock, T. H.) 363–383 (Univ. Chicago Press, 1988).
6. Brown, E. W., Yuhki, N., Packer, C. & O'Brien, S. J. *J. Virol.* **68**, 5953–5968 (1994).
7. Gilbert, D. A., Packer, C., Pusey, A. E., Stephens, J. C. & O'Brien, S. J. *J. Hered.* **82**, 378–386 (1991).
8. Wildt, D. E. *et al. Nature* **329**, 328–331 (1987).
9. Appel, M. J. G. *Virus Infections in Carnivores* (ed. Appel, M. J. G.) 133–160 (Elsevier, Amsterdam, 1987).
10. Appel, M. J. G. *et al. J. vet. diagnost. Invest.* **6**, 277–288 (1994).
11. Orvell, C., Sheshberadaran, H. & Norrby, E. *J. Virol.* **66**, 443–456 (1985).
12. Appel, M. J. G. & Robson, D. S. *Am. J. vet. Res.* **34**, 1459–1463 (1973).
13. Appel, M. J. G., Pearce-Kelling, S. & Summers, B. A. *J. vet. diagnost. Invest.* **4**, 258–263 (1992).
14. Montali, R. J., Bartz, C. R. & Bush, M. *Virus Infections of Carnivores* (ed. Appel, M.) 437–443 (Elsevier, Amsterdam, 1991).
15. Brown, E. W., Miththapala, S. & O'Brien, S. O. *J. Zool. Wildl. Med.* **24**, 357–364 (1993).
16. Carmichael, L. E., Joubert, J. C. & Pollack, R. V. *H. Am. J. vet. Res.* **41**, 784–791 (1980).
17. Hofer, H. & East, M. L. *Symp. zool. Soc. London* **65**, 347–366 (1993).
18. Barrett, T. *et al. Virology* **193**, 1010–1012 (1993).
19. Swafford, D. L. *Phylogenetic Analysis Using Parsimony (PAUP)* (Illinois Natural History Survey, Champaign, IL, 1984).
20. Felsenstein, J. *Phylogeny Inference Package (PHYLP)*, Version 3.3 (University of Washington, Seattle, WA, 1995).

ACKNOWLEDGEMENTS. We thank M. Grob and M. Elgizoli for viral antigens, and M. East and H. Hofer for providing two hyaena carcasses. This work was supported in part by the Messeri Foundation of Zurich, the University of Tennessee, Cornell University, Smithsonian NOAHS Center, the National Science Foundation, National Geographic, and British Airways.

A common molecular basis for three inherited kidney stone diseases

Sarah E. Lloyd*, Simon H. S. Pearce*,
Simon E. Fisher†, Klaus Steinmeyer‡,
Blanche Schwappach‡, Steven J. Scheinman*§,
Brian Harding*, Alessandra Bolino||,
Marcella Devoto||, Paul Goodyer¶, Susan P. A.
Rigden#, Oliver Wrong*, Thomas J. Jentsch‡,
Ian W. Craig† & Rajesh V. Thakker*††

* MRC Molecular Endocrinology Group, Royal Postgraduate Medical School, Hammersmith Hospital, Du Cane Road, London W12 0NN, UK

† Genetics Laboratory, University of Oxford, South Parks Road, Oxford OX1 3QU, UK

‡ Centre for Molecular Neurobiology Hamburg (ZMNH), Hamburg University, Martinistrasse 52, D-20246 Hamburg, Germany

§ Department of Medicine, State University of New York Health Science Center, Syracuse, New York 13210, USA

|| Laboratorio di Genetica Molecolare, Istituto G. Gaslini, Largo Gaslini 5, 16148 Genova, Italy

¶ L'Hôpital de Montreal pour Enfants, 2300 rue Tupper, A717 Montreal, Quebec H3H1P3, Canada

Department of Paediatric Nephrology, Guy's Hospital, St Thomas's Street, London SE1 9RT, UK

* Department of Nephrology, The Middlesex Hospital, Mortimer Street, London W1N 8AA, UK

KIDNEY stones (nephrolithiasis), which affect 12% of males and 5% of females in the western world, are familial in 45% of patients^{1,2} and are most commonly associated with hypercalciuria¹. Three disorders of hypercalciuric nephrolithiasis (Dent's disease³, X-linked recessive nephrolithiasis (XRN)⁴, and X-linked recessive hypophosphataemic rickets (XLRH)⁵) have been mapped to Xp11.22 (refs 5–7). A microdeletion⁶ in one Dent's disease kindred allowed the identification of a candidate gene, *CLCN5* (refs 8,9) which encodes a putative renal chloride channel. Here we report the investigation of 11 kindreds with these renal tubular disorders for *CLCN5* abnormalities; this identified three nonsense, four missense and two donor splice site

mutations, together with one intragenic deletion and one microdeletion encompassing the entire gene. Heterologous expression of wild-type *CLCN5* in *Xenopus* oocytes yielded outwardly rectifying chloride currents, which were either abolished or markedly reduced by the mutations. The common aetiology for Dent's disease, XRN and XLRH indicates that *CLCN5* may be involved in other renal tubular disorders associated with kidney stones.

Analysis of *CLCN5* reverse transcriptase–polymerase chain reaction (RT–PCR) products encompassing the entire 2238-bp coding sequence⁹ from probands of 11 kindreds with Dent's disease, XRN and XLRH, revealed different *CLCN5* mutations (Table 1 and Fig. 1). Each mutation was confirmed and demonstrated to cosegregate with the disease by using genomic DNA together with the appropriate PCR primers and restriction enzymes, or by sequence-specific oligonucleotide (SSO) probe analysis (Table 1 and Fig. 2). In addition, the absence of these *CLCN5* abnormalities in 110 alleles from 69 (28 males and 41 females) unrelated, normal individuals established that they were not common polymorphisms. *CLCN5* belongs to a family of voltage-gated chloride-channel genes (*CLCN1* to *CLCN5* and *CLCN-Ka* and *Kb*), which encode proteins (CLC-1 to CLC-5, CLC-Ka and CLC-Kb) that have about 12 transmembrane domains¹⁰. These chloride channels are important for the control of membrane excitability, transepithelial transport, and possibly regulation of cell volume¹⁰. However, mutations have been identified previously in only *CLCN1*, which is expressed in muscle¹¹ and is associated with myotonia congenita^{12–14}. Thus, to assess further the functions of CLC-5 and its mutations, we performed heterologous expression studies in *Xenopus* oocytes. Expression of the human wild-type (WT) CLC-5 reproducibly yielded strongly outwardly rectifying, essentially time-independent currents (Fig. 3). Ion substitution experiments indicated that these were carried by anions, with a chloride > iodide conductance sequence (Fig. 3b,c), as is the case with other chloride channels (CLC-0, CLC-1 and CLC-2) of this family^{12,15,16}. However, these human CLC-5 currents, which were indistinguishable from those of rat CLC-5 (ref. 17), differed from the others in being strongly outwardly rectifying and in being observed only at potentials more positive than +10 mV. Although positive potentials of even +40 mV have been observed in apical membranes of some actively transporting epithelia¹⁸, we are not aware of renal cells where these voltages would be reached *in vivo*. CLC channels are known to function as multimeric complexes, which are most likely to be tetramers¹², and it seems possible that CLC-5 forms hetero-oligomers with as yet unknown subunits *in situ* that may render the channels open at a more physiological voltage. Our functional expression of CLC-5 provides a valuable means of investigating this further and in assessing the functional effects of the CLC-5 mutations.

Expression of the four missense and three nonsense mutations (Table 1), and the in-frame deletion of the predicted transmembrane domain D2 (Fig. 1), abolished the CLC-5 currents or reduced them (S244L and S520P) to levels where they were difficult to distinguish from endogenous oocyte currents (Fig. 3d,f). As a control, we also expressed more conservative changes at codons 244 and 520; S244T, S520T, S244A and S520A all elicited chloride currents that were similar to the WT (data not shown). Thus, the mutations found in the hypercalciuric nephrolithiasis pedigrees grossly and specifically affect CLC-5 function, thereby strongly suggesting a causal role in the disease. Dent's disease, which is characterized by low-molecular-weight proteinuria (LMWP), hypercalciuria, nephrocalcinosis, nephrolithiasis, rickets and eventual renal failure^{3,6}, has phenotypic similarities to XRN^{4,7} and XLRH⁵ (Fig. 2). However, there are important differences, as rickets is absent in XRN, and nephrocalcinosis and moderate renal failure are more notable in XLRH. A correlation between these phenotypic differences, the different mutations (Table 1 and Fig. 1) and the resulting abnormal chloride currents (Fig. 3) could not be established. Thus, Dent's disease was found to be associated with the mutations W279X,

††To whom correspondence should be addressed.

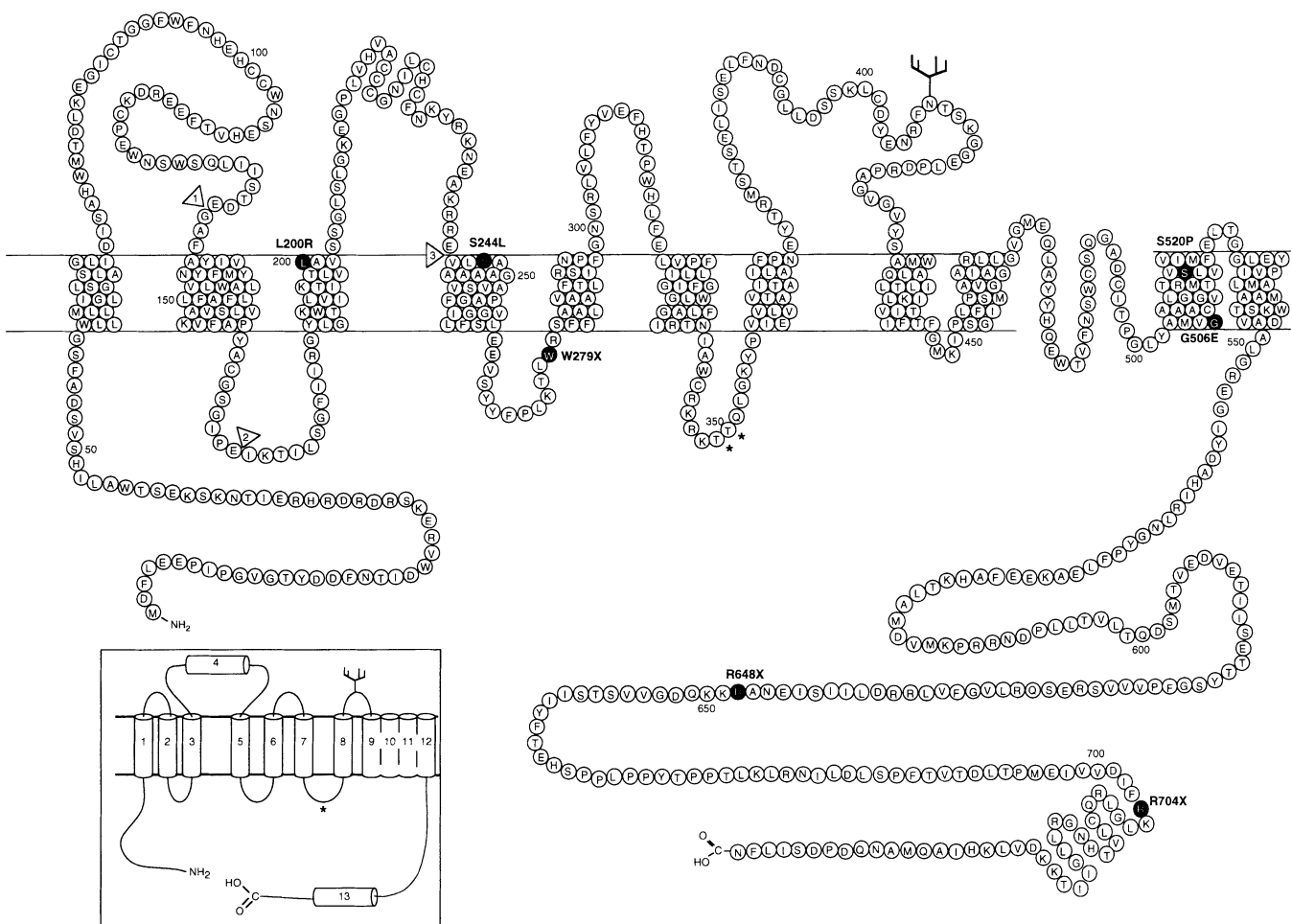


FIG. 1 Schematic representation of a predicted topology of CLC-5, based on the reported DNA sequence⁹, to illustrate the mutations associated with X-linked hypercalcaemic nephrolithiasis. The mutations found in 11 families with X-linked hypercalcaemic nephrolithiasis (Table 1) are shown with the amino acid highlighted in black and the codon and substituted amino acid shown alongside. Arrows 1 and 2 delineate the amino acids predicted to be deleted in families 19/94 and 4/94, and arrows 1–3 delineate those deleted in family 7.1/94 (Table 1). Every 50th amino acid of the 746-amino acid CLC-5 protein and the consensus phosphorylation (asterisk) and glycosylation (branch) sites at codons 349, 350 and 408, respectively, are indicated. The correct topology for the CLC channels is unknown and the predicted topology of the CLC-5 putative transmembrane domains (D1–D13) has been revised⁹ and is based upon a model^{10,15} (inset) that places

R648X, L200R, S520P, two microdeletions and two donor splice site mutations; XRN was associated with R704X and G506E; and XLRH was associated with S244L. In addition, the markedly reduced, but not abolished, chloride currents associated with S244L were not specific for XLRH as they were also associated with S520P in Dent's disease (Fig. 3f), and the undetectable chloride currents associated with all the other mutations (Fig. 3) were found in XRN and Dent's disease. As may be expected for a channel protein, all the disease-causing missense mutations were confined to the predicted transmembrane domains (Fig. 1 and Table 1). In addition, the R648X and R704X mutations, which predict a loss of 100 and 42 amino acids from the cytoplasmic carboxy terminus (Fig. 1), delete domain D13, which is conserved in all eukaryotic CLC proteins, including the one of *Saccharomyces cerevisiae*¹⁹. This suggests that D13 and the C-terminal region play an important but as yet unspecified role. The donor splice site mutations (Fig. 2 and Table 1), which are associated with a loss of exon 5, lead to an in-frame deletion of the predicted transmem-

D4 extracellularly, and in which the hydrophobic core of the D9–D12 region crosses the membrane 3 or 5 times and contains a hydrophilic region (codons 481–502), the precise location of which remains unknown. An alternative model placing D2 extracellularly has also been proposed^{20,21}, but the donor splice site mutations in families 4/94 and 19/94 that result in the loss of codons 132–172 (arrows 1 and 2) indicate the importance of this segment and provide support for a transmembrane location of D2. The 28 amino acids (codons 700–728) represent a conserved region that has been designated domain D13. The R704X mutation in D13 highlights the importance of this region, the function of which remains to be defined. The nonsense and donor splice site mutations were found to involve the loops and intracellular regions, whereas all the missense mutations occurred within the transmembrane spans.

brane domain D2 (Fig. 1). A splice variant of rCLC-K2, deleted for D2, was reported to yield chloride currents indistinguishable from those of WT rCLC-K2 (ref. 20), and it was therefore proposed that D2 does not cross the membrane²¹. However, our findings provide further support for a functional role and transmembrane location for D2.

Our results indicate that CLC-5 is a chloride channel whose functional loss results surprisingly in a renal tubulopathy that is associated with LMWP, hypercalcaemia and nephrolithiasis. The resorption of filtered protein occurs almost exclusively in the proximal tubule, whereas that of calcium occurs in the proximal tubule, the thick ascending limb of Henle's loop, and the distal nephron²². Thus, further investigations of *CLCN5* expression along the human nephron, and of the mechanisms whereby *CLCN5* mutations lead to LMWP and hypercalcaemia, will lead to increased understanding of renal tubular function and pathology. In addition, our findings, which have defined a common molecular pathology of *CLCN5* in three disorders of hereditary

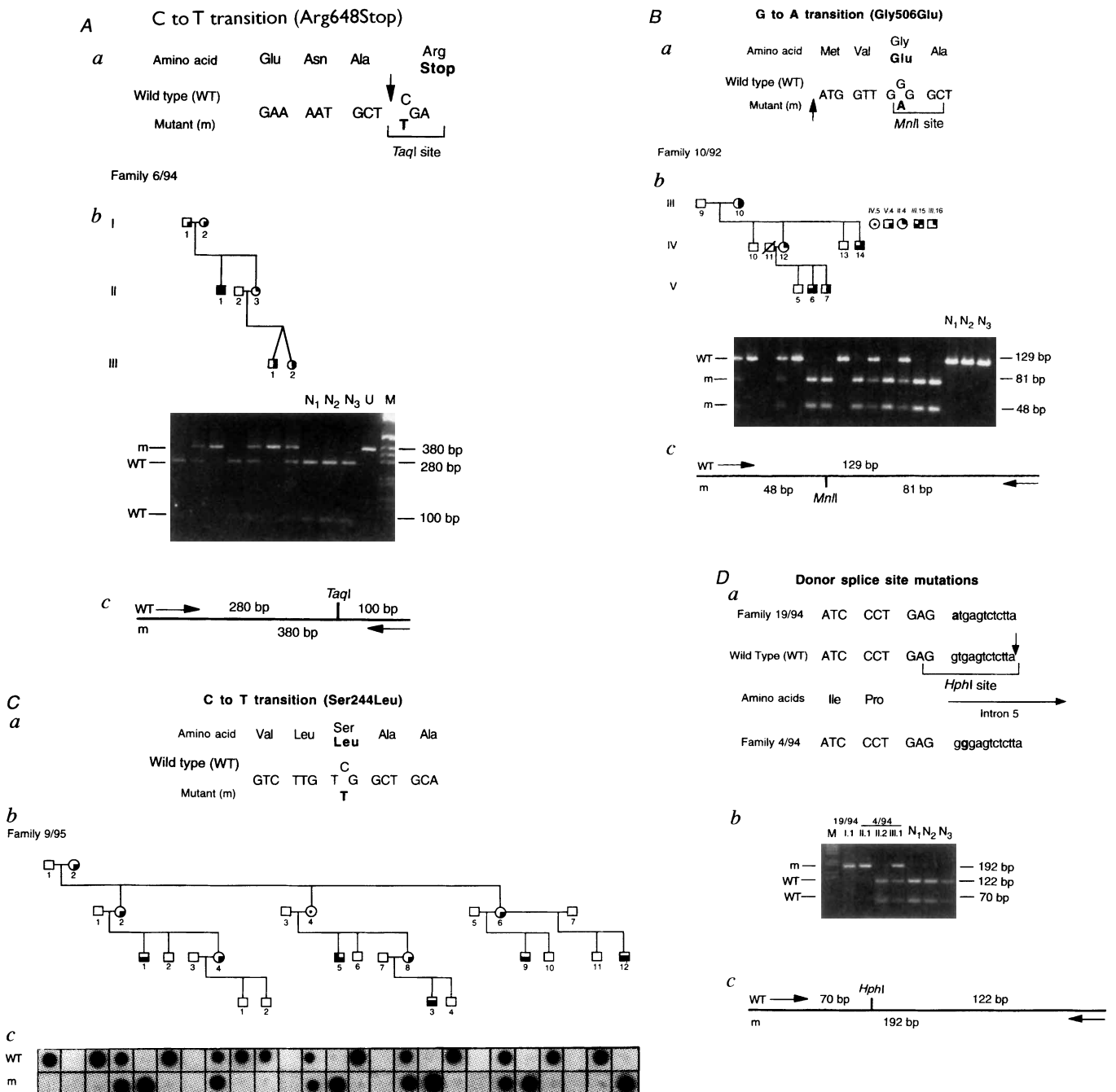


FIG. 2 Detection of CLC-5 mutations by restriction enzyme (A, B, D) and SSO analysis (C). Families with Dent's disease (4/94, 6/94 and 19/94), XRN (10/92) and XLRH (9/95) are shown with LMWP, hypercalciuria, nephrocalcinosis and nephrolithiasis, end-stage renal failure, and carrier female. Only 13 of the 102 members of the six-generation XRN family 10/92 are shown with the individual identification as reported⁶. Family 9/95 (XLRH) has not been assessed for LMWP but III.1, III.5, III.9, III.12 and IV.3 have proteinuria, and III.1 and III.9 have moderate renal failure (creatinine clearance, 60–65 ml min⁻¹ m⁻²)⁵. In family 4/94 (D), II.1 is the affected father, II.2 the unaffected mother, and III.1 the affected daughter. DNA sequence abnormalities, together with their encoded amino acids (a) cosegregation of the mutation with the disease in each family (b), and restriction maps of the wild-type (WT) and mutant (m) sequences (c) are shown. These mutations were not present in 69 unrelated normal individuals (N₁₋₃ shown). Mutant RT-PCR products (192 bp) that differed from WT by 123 bp, which is the size of exon 5, were obtained in families 19/94 and 4/94. This exon skipping resulted from donor splice site mutations and analysis of the exon (upper-case letters) 5–intron (lower-case letters) 5 boundary revealed a g to a transition at position +1 in family 19/94, and t to g transversion at position +2 in family 4/94 (D).

METHODS. RNA was extracted from an Epstein–Barr virus-transformed lymphoblastoid cell line obtained from peripheral blood cells of each proband using methods published previously²³. RT–PCR was performed using pairs of nested CLCN5-specific primers and the following conditions: 25 cycles of denaturation at 94 °C, annealing at 60 °C and extension at 72 °C, each for 30 s. The PCR products were gel purified and the DNA sequences of both strands determined by Taq polymerase cycle sequencing and a semi-automated detection system (ABI-373 sequencer) as described previously²⁴. Genomic DNA, restriction enzyme and SSO studies were performed as described previously²⁵.

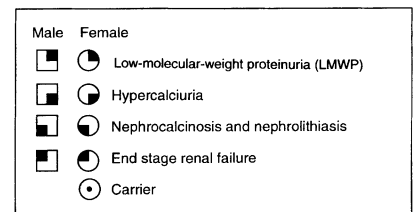


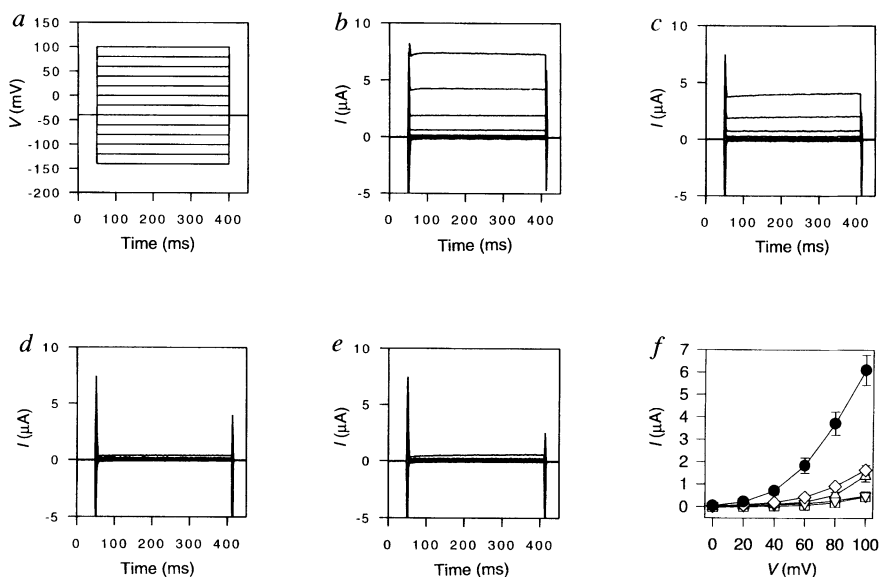
TABLE 1 CLCN5 mutations found in families with X-linked hypercalcaemic nephrolithiasis

Family	Codon	Base change	Amino acid change	Restriction enzyme change/SSO	Predicted effect
Nonsense mutations					
7.2/94*	279	TGG → TGA	Trp → Stop	Maelll	Loss of 469 amino acids from D6 to C terminus
6/94*	648	CGA → TGA	Arg → Stop	TaqI	Loss of 100 amino acids from cytoplasmic domain
12/95†	704	CGA → TGA	Arg → Stop	BsII	Loss of 42 amino acids from cytoplasmic domain
Missense mutations					
13/94*	200	CTG → CGG	Leu → Arg	Acil	Disruption of charge distribution within D3
9/95‡	244	TCG → TTG	Ser → Leu	SSO	Disruption of helix in D5
10/92†	506	GGG → GAG	Gly → Glu	MnlI	Disruption of charge distribution within D11
2/92*	520	TCT → CCT	Ser → Pro	MnlI	Disruption of helix in D11
Splice site mutations					
4/94*	Intron 5 132–172 deleted	gt → gg		HphI	Loss of D2
19/94*	Intron 5 132–172 deleted	gt → at		HphI	Loss of D2
Deletions					
7.1/94*	2-kb deletion 132–241 deleted				Loss of D2–D4
12/89*§	515-kb deletion				Absence of protein

* Eight British families (26 affected, 33 unaffected members) with Dent's disease, † two North American families (29 affected, 75 unaffected members) with XRN, and ‡ one Italian family (9 affected, 10 unaffected members) with XLRH were studied. The clinical details of 7 of the 8 kindreds with Dent's disease, designated families 2/92, 4/94, 6/94, 7.2/94, 12/89, 13/94 and 19/94 have been previously reported³ and referred to as families A, E, D, F, H, C and G, respectively.

§ Previously described^{6,8}.

FIG. 3 Electrophysiological analysis of *Xenopus* oocytes expressing human CLC-5 and its mutants. **a**, The pulse protocol for voltage-clamping, in which oocytes were sequentially clamped from a holding potential of -40 mV to voltages between $+100$ and -140 mV for 350 ms in steps of 20 mV. **b**, The resulting current traces from an oocyte expressing WT CLC-5, measured in ND96 (104 mM chloride), and **c**, in ND96 in which 80 mM Cl^- was replaced by I^- . The resulting strongly outwardly rectifying anion current is reduced by partial replacement of Cl^- by I^- . **d**, Current traces from a mutant in which the exon encoding domain D2 (Fig. 1) is deleted in frame (Table 1 and Fig. 2); currents did not differ from water-injected control oocytes (**e**). **f**, Current–voltage relationships showing currents (measured in ND96) of WT CLC-5 (filled circles) and the missense mutants L200R (inverted triangles), S244L (triangles), G506E (squares) and S520P (diamonds). Currents are averaged from several oocytes, and error bars indicate standard error of the mean (s.e.m.) Because CLC-5 is strongly outwardly rectifying, only currents at positive voltages are shown. Although L200R and G506E currents are not different from uninjected control oocytes, mutants S244L and S520P elicit strongly reduced, but detectable, currents. Currents with nonsense mutants (W279X, R648X, R704X) were not different from negative controls (data not shown). Averaged currents at $+80$ mV ($\mu\text{A} \pm \text{s.e.m.}$, n , number of oocytes) were determined to be: WT, 3.71 ± 0.51 , $n = 17$; uninjected control, 0.27 ± 0.03 , $n = 19$; L200R, 0.19 ± 0.03 , $n = 4$; S244L, 0.54 ± 0.12 , $n = 6$; G506E, 0.27 ± 0.02 , $n = 12$; S520P, 0.92 ± 0.11 , $n = 12$; W279X, 0.23 ± 0.02 , $n = 10$; R648X, 0.32 ± 0.08 , $n = 3$; R704X, 0.26 ± 0.03 , $n = 7$; deletion of D2, 0.23 ± 0.03 , $n = 4$. **METHODS**. After engineering an *Nco*I site at the initiator methionine, a cDNA encoding CLC-5 was inserted into the *Nco*I site of the expression vector, PTLN, containing *Xenopus* globin untranslated regions²⁶. Mutations



were introduced by recombinant PCR and sequenced. Capped RNA was transcribed from the linearized construct using SP6 RNA polymerase. About 10 ng of cRNA was injected into *Xenopus* oocytes prepared and handled as described previously²⁷. After 2–3 days at 16 °C, oocytes were examined at room temperature by standard two-electrode voltage-clamp technique. Standard extracellular solution was ND96 (96 mM NaCl, 2 mM KCl, 1.8 mM CaCl_2 , 1 mM MgCl_2 , 5 mM HEPES, pH 7.4), or ND96 in which part of the NaCl was replaced by NaI. For every construct, we used three different batches of cRNAs and at least three different batches of oocytes, always with similar results. In addition, the translatability of cRNA was confirmed by *in vitro* translation.

nephrolithiasis, indicate that CLC-5 and possibly other renal chloride channels, may be implicated in other disorders associated with renal stones, which account for up to 1% of all hospital admissions². □
Note added in proof: Two additional genes (*CLCN6* and *CLCN7*) encoding the putative chloride channels CLC-6 and CLC-7 have also recently been cloned²⁸.

Received 13 October; accepted 18 December 1995.

- Coe, F. L., Parks, J. H. & Asplin, J. R. *New Engl. J. Med.* **327**, 1141–1152 (1992).
- Smith, L. H. *J. Urol.* **141**, 707–710 (1989).
- Wrong, O. M., Norden, A. G. W. & Feest, T. G. Q. *J. Med.* **87**, 473–493 (1994).
- Frymoyer, P. A. et al. *New Engl. J. Med.* **325**, 681–686 (1991).
- Bolino, A. et al. *Eur. J. hum. Genet.* **1**, 269–279 (1993).
- Pook, M. A. et al. *Hum. molec. Genet.* **2**, 2129–2134 (1993).
- Scheinman, S. J. et al. *J. clin. Invest.* **91**, 2351–2357 (1993).
- Fisher, S. E. et al. *Hum. molec. Genet.* **3**, 2053–2059 (1994).
- Fisher, S. E. et al. *Genomics* **29**, 598–606 (1995).
- Jentsch, T. J., Günther, W., Pusch, M. & Schwappach, B. *J. Physiol., Lond.* **482**, 19S–25S (1995).
- Steinmeyer, K., Ortland, C. & Jentsch, T. J. *Nature* **354**, 301–304 (1991).
- Steinmeyer, K. et al. *EMBO J.* **13**, 737–743 (1994).
- Meyer-Kleine, C., Steinmeyer, K., Ricker, K., Jentsch, T. J. & Koch, M. C. *Am. J. hum. Genet.* **57**, 1325–1334 (1995).
- Koch, M. C. et al. *Science* **257**, 797–800 (1992).
- Pusch, M., Ludewig, U., Rehfeldt, A. & Jentsch, T. J. *Nature* **373**, 527–531 (1995).
- Thiemann, A., Gründer, S., Pusch, M. & Jentsch, T. J. *Nature* **356**, 57–60 (1992).
- Steinmeyer, K., Schwappach, B., Bens, M., Vandewalle, A. & Jentsch, T. J. *J. biol. Chem.* **270**, 31172–31177 (1995).
- Higgins, J. T., Gebler, B. & Frömter, E. *Pflügers Arch. Eur. J. Physiol.* **371**, 87–97 (1977).
- Green, J. R., Brown, N. H., DiDomenico, B. J., Kaplan, J. & Eide, D. J. *Molec. gen. Genet.* **241**, 542–553 (1993).
- Adachi, S. et al. *J. biol. Chem.* **269**, 17677–17683 (1994).
- Middleton, R. E., Pheasant, D. J. & Miller, C. *Biochemistry* **33**, 13189–13198 (1994).
- Friedman, P. A. & Gesek, F. A. *Physiol. Rev.* **75**, 429–471 (1995).
- Sambrook, J., Fritsch, E. F. & Maniatis, T. *A Laboratory manual 2nd edn.* 7.19–7.22 (Cold Spring Harbor Laboratory Press, New York, 1989).
- Pearce, S. H. S. et al. *J. clin. Invest.* **96**, 2683–2692 (1995).
- Thakker, R. V. et al. *J. clin. Invest.* **91**, 2815–2821 (1993).
- Krieg, P. A. & Melton, D. A. *Nucleic Acids Res.* **12**, 7057–7070 (1984).
- Jentsch, T. J., Steinmeyer, K. & Schwarz, G. *Nature* **348**, 510–514 (1990).
- Brandt, S. & Jentsch, T. J. *FEBS Lett.* **377**, 15–20 (1995).

ACKNOWLEDGEMENTS. We thank D. Schlessinger and G. Williams for discussions; B. Farren for collection of samples; A. G. W. Norden for urine analysis; C. Zoccali and G. Romeo for access to the Italian family; and J. Walls for access to one of the British families. S.H.S.P. is an MRC Training Fellow. This work was supported by the Medical Research Council (S.E.L., S.H.S.P., B.H. and R.V.T.), the Human Genome Mapping Project, UK (S.E.F. and I.W.C.), the Deutsche Forschungsgemeinschaft (T.J.J. and K.S.) and the American Heart Association (S.J.S.).

Preferential activation of midbrain dopamine neurons by appetitive rather than aversive stimuli

Jacques Mirenowicz* & Wolfram Schultz†

Institute of Physiology, University of Fribourg, CH-1700 Fribourg, Switzerland

MIDBRAIN dopamine systems are crucially involved in motivational processes underlying the learning and execution of goal-directed behaviour^{1–5}. Dopamine neurons in monkeys are uniformly activated by unpredicted appetitive stimuli such as food and liquid rewards and conditioned, reward-predicting stimuli. By contrast, fully predicted stimuli are ineffective^{6–8}, and the omission of predicted reward depresses their activity⁹. These characteristics follow associative-learning rules^{10,11}, suggesting that dopamine responses report an error in reward prediction¹². Accordingly, neural network models are efficiently trained using a dopamine-like reinforcement signal^{13,14}. However, it is unknown whether the responses to environmental stimuli concern specific motivational attributes or reflect more general stimulus salience^{4,15}. To resolve this, we have compared dopamine impulse responses to motivationally opposing appetitive and aversive stimuli. In contrast to appetitive events, primary and conditioned non-noxious aversive stimuli either failed to activate dopamine neurons or, in cases of close resemblance with appetitive stimuli, induced weaker

responses than appetitive stimuli. Thus, dopamine neurons preferentially report environmental stimuli with appetitive rather than aversive motivational value.

Two monkeys were instrumentally conditioned with visual and auditory stimuli. Appetitive conditioned stimuli eliciting lever pressing for a juice reward alternated randomly with aversive conditioned stimuli inducing hand withdrawal from a resting key in order to avoid a mild air puff to the hand or hypertonic saline to the mouth. Appetitive and aversive stimuli were adjusted to comparable motivational strength by setting juice drop size, air pressure and saline drop size slightly above a threshold below which task performance dropped sharply. Task performance was >90–95% correct. Outside the task, animals were presented with free juice drops but not with air puffs or hypertonic saline, which rapidly disrupted their collaboration.

We used two monkeys to record from dopamine neurons in midbrain catecholamine cell groups A8 (23 neurons dorsal to lateral substantia nigra), A9 (251 neurons in pars compacta of substantia nigra) and A10 (40 neurons in ventral tegmental area); we distinguished these from other midbrain neurons by their distinctive electrophysiological characteristics, which consisted of polyphasic, relatively long discharges occurring at comparatively low frequencies^{6–8,10}. Most dopamine neurons were phasically activated by primary and conditioned appetitive stimuli at short mean latencies of 93–115 ms, thus confirming earlier results^{6–8} (conditioned light: 100 of 128 neurons, 78%; conditioned sound: 120 of 158 neurons, 76%; free juice: 62 of 80 neurons, 78%). In contrast, very few dopamine neurons were activated by aversive stimuli, such as a conditioned sound for air puff (1 of 31 neurons, 3%), light for air puff (8 of 56 neurons, 14%) or fractal picture for saline (4 of 30 neurons, 13%) (Fig. 1). The total of 13 neurons activated by conditioned aversive stimuli belonged to groups A8 (5 of 12 neurons), A9 (7 of 89) and A10 (1 of 16), suggesting a potential mediolateral gradient for the few aversive responses. These few aversive responses failed to result in an average population response (Fig. 3b, d right). The infrequent primary aversive air puff activated only 7 of 51 neurons (14%), all of them being in A9 (Fig. 2). Sixteen of the total 20 neurons with aversive responses also showed appetitive responses. The low responsiveness to aversive stimuli cannot be attributed to movement differences which have been shown not to influence dopamine neurons^{7,17,18}. Conditioned aversive stimuli elicited depressions in 36 of 117 neurons (31%; Fig. 1, bottom), reminiscent of depressions related to the omission of expected reward⁹.

The chronology of experiments demonstrates the way dopamine neurons were preferentially activated by appetitive stimuli. The first animal was extensively conditioned with a small light for appetitive outcome. Later, an adjacent, similar light of a different colour served as the aversive stimulus associated with air-puff avoidance and alternated randomly with the appetitive light, the animal discriminating well between them. Dopamine neurons discriminated quantitatively between these motivationally opposing stimuli, the appetitive light activating the majority of them whereas the similar aversive light activated fewer neurons and at lower magnitudes (Fig. 3a). In order to distinguish between genuinely, albeit lower, aversive responsiveness and confounding generalization to appetitive stimuli, we subsequently conditioned an auditory aversive stimulus previously not associated with appetitive outcome. As already described, only 1 of 31 neurons was activated by the aversive sound (Fig. 3b), suggesting that the aversive activations of Fig. 3a were due to stimulus generalization. In a third step, we tested the general effectiveness of auditory stimuli by reversing stimulus modalities and indeed found most neurons to be activated by the appetitive sound (Fig. 3c). Although behavioural response to the appetitive light had been extinguished, the similar aversive light was still effective, albeit with many fewer neurons and at lower response magnitude. This responsiveness may either suggest a remaining appetitive 'tag' on visual stimuli or a general visual response preference. When testing this, we avoided stimulus generalization by presenting

* Present address: Department of Experimental Psychology, University of Cambridge, Cambridge CB2 3EB, UK.
 † To whom correspondence should be addressed.